

IECAG
2021



CLASSIFICATION OF HYPERSPECTRAL IMAGES WITH CNN IN AGRICULTURE AND FORESTRY

EREN CAN SEYREK^{1,*} AND MURAT UYSAL^{1,2}

¹ DEPARTMENT OF GEOMATICS ENGINEERING, AFYON KOCATEPE UNIVERSITY, 03200 AFYONKARAHISAR, TURKEY

² REMOTE SENSING AND GIS RESEARCH AND APPLICATION CENTER, AFYON KOCATEPE UNIVERSITY, 03200 AFYONKARAHISAR, TURKEY

CONTENTS

- 1. INTRODUCTION**
- 2. CLASSIFICATION METHODS**
- 3. DATA SETS**
- 4. RESULTS**
- 5. CONCLUSIONS**

1. INTRODUCTION

- Remote sensing data obtained from airborne and spaceborne sensors are become provide more detailed spatial and spectral resolution with the developments in recent years.
- Remote sensing is a time-saving and low-cost alternative to precision agriculture and forestry applications like detecting and separating various vegetation species.
- Hyperspectral images (HSI) are the most suitable remote sensing data for these analyses, by providing high spectral resolution with hundreds of spectral bands.

- HSI's high spectral information reveals a huge volume of data and high dimensionality.
- This causes Hughes phenomenon which is one of main problems in HSI classification problems [1].
- Traditional classifiers such as Maximum Likelihood and Spectral Angle Mapper cannot handle HSI data with high classification accuracy.
- In the last three decades, various studies have been conducted to apply the high classification success of Machine Learning (ML) methods to HSI classification problems [2-3].

1. Dalponte, M., et al., *The Role of Spectral Resolution and Classifier Complexity in the Analysis of Hyperspectral Images of Forest Areas*. *Remote Sensing of Environment*, 2009. 113(11): p. 2345-2355.
2. Gualtieri, J., et al. *Support Vector Machine Classifiers as Applied to AVIRIS Data*. in *Proc. Eighth JPL Airborne Geoscience Workshop*. 1999. Pasadena.
3. Chan, J.C.-W. and D. Paelinckx, *Evaluation of Random Forest and Adaboost Tree-based Ensemble Classification and Spectral Band Selection for Ecotope Mapping Using Airborne Hyperspectral Imagery*. *Remote Sensing of Environment*, 2008. 112(6): p. 2999-3011.

- In recent years, Convolutional Neural Network (CNN) algorithms that have become more widespread on various application fields, has been used in the HSI classification.
- Several CNN architectures were designed for classifying HSI accurately [4-5].
- In this study, we compared the classification accuracy of CNN and well-known Support Vector Machines (SVM).
- For this purpose, we used two publicly available data sets named Salinas Scene and HyRANK Loukia, that contains vegetation species classes.
- We evaluated classification performances by examining overall accuracy, producer and user accuracy, f scores, and kappa coefficient (κ) respectively.

4. Luo, Y., et al. *HSI-CNN: A Novel Convolution Neural Network for Hyperspectral Image*. in 2018 International Conference on Audio, Language and Image Processing (ICALIP). 2018. Beijing: IEEE.

5. Roy, S.K., et al., *HybridSN: Exploring 3-D-2-D CNN Feature Hierarchy for Hyperspectral Image Classification*. *IEEE Geoscience and Remote Sensing Letters*, 2019. 17(2): p. 277-281.

2. CLASSIFICATION METHODS

1. Support Vector Machines (SVM)

- SVM is a supervised and non-parametric ML algorithm based on statistical learning theory, developed by Vapnik [6].
- The main approach of SVM is to find the best decision boundary that minimizes generalization error, called as optimum hyperplane [7, 8].
- Data samples that are closest to the hyperplane were used to measure the margin, called as support vectors (SV) [7].

6. Cortes, C. and V. Vapnik, *Support-Vector Networks*. *Machine Learning*, 1995. 20(3): p. 273-297.

7. Vapnik, V., *The Nature of Statistical Learning Theory*. 1995, New York: Springer - Verlag. 188.

8. Pal, M. and P. Mather, *Support Vector Machines for Classification in Remote Sensing*. *International Journal of Remote Sensing*, 2005. 26(5): p. 1007-1011.

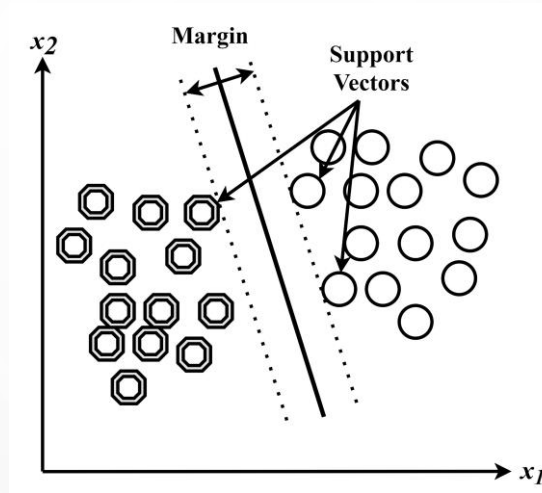


Figure 1. Optimum hyperplane and support vectors in the SVM.

- In most classification problems, kernel functions are used to transform the data into higher dimensional feature space for separate classes with linear functions.
- We used the RBF kernel when implementing the SVM model, by determining C and γ parameters with the grid search.

2. Convolutional Neural Networks (CNN)

- CNN is a form of deep learning that processes data in the form of multiple arrays such as, 1D data including sequences and signals, 2D data including images and audio spectrograms, 3D data including volumetric images and videos [13].
- CNNs are generally formed of three fundamental components with serves different purposes:
 - convolution layer
 - pooling layer
 - fully connected layer

13. LeCun, Y., Y. Bengio, and G. Hinton, *Deep Learning. Nature*, 2015. 521(7553): p. 436-444.

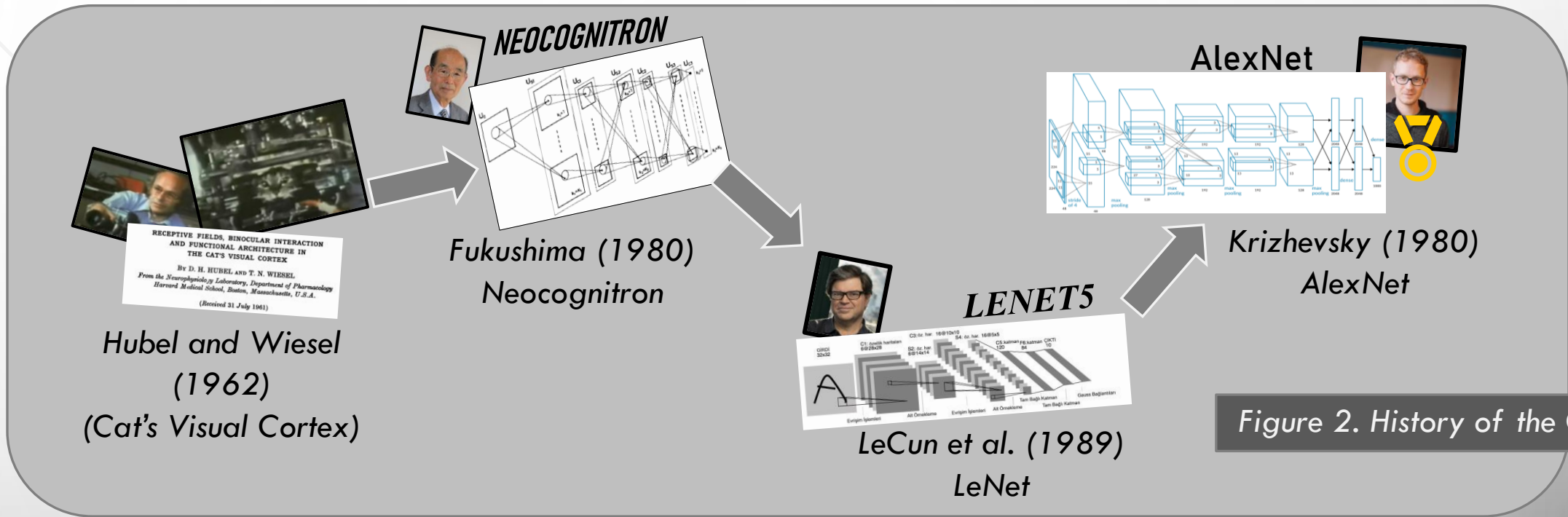
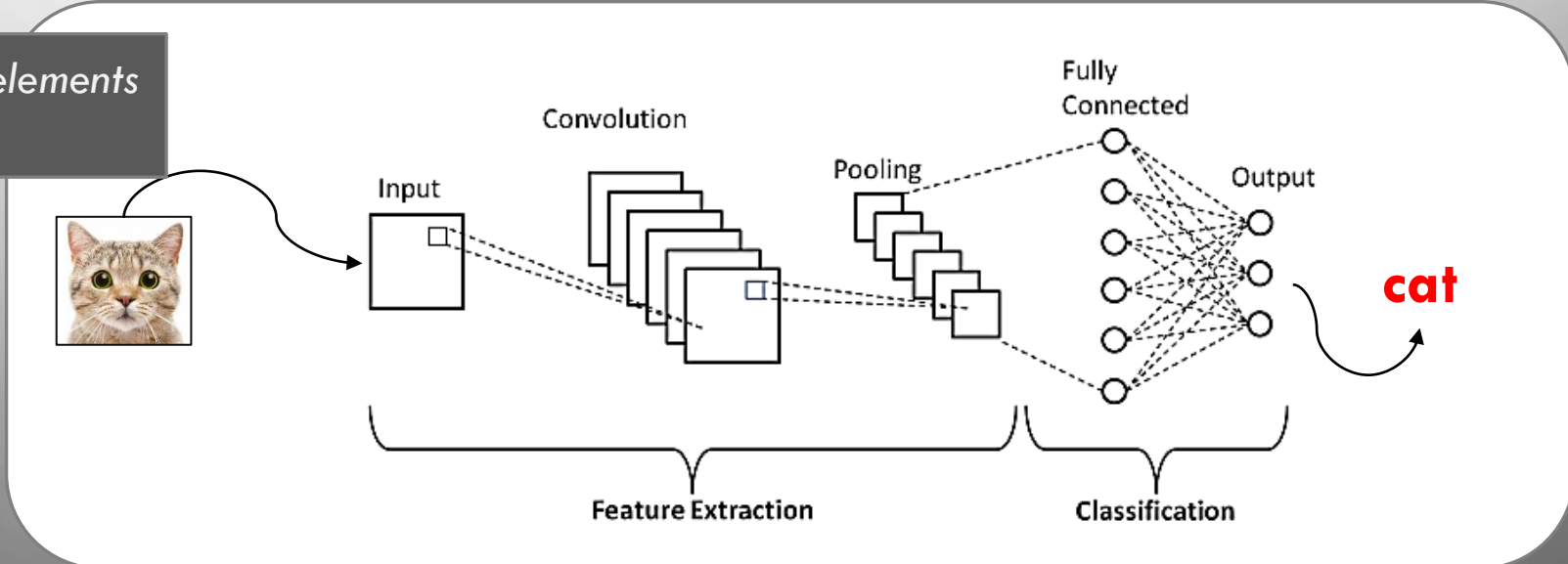


Figure 3. Fundamental elements of the CNN.



- To classify HSIs, we used a hybrid CNN model with two 3D and one 2D convolution layers that can extract spectral and spatial features along bands.
- To avoid spectral redundancy of HSI, we applied PCA along bands and we used the first 15 principal components.
- We selected PReLU activation function for its advantages over ReLU.
- All weights are randomly initialized and trained using back-propagation algorithm with the Adam optimizer by using the softmax classifier.
- We selected epoch and batch size parameters as 256 and 500 respectively.

3. DATA SETS

1. Salinas Scene

- Acquired on 1998 by AVIRIS sensor with a 3.7-meter spatial resolution and 224 bands.
- To train the algorithms, we selected 150 samples from each class randomly.
- Final size of the hypercube is $512 \times 217 \times 204$.

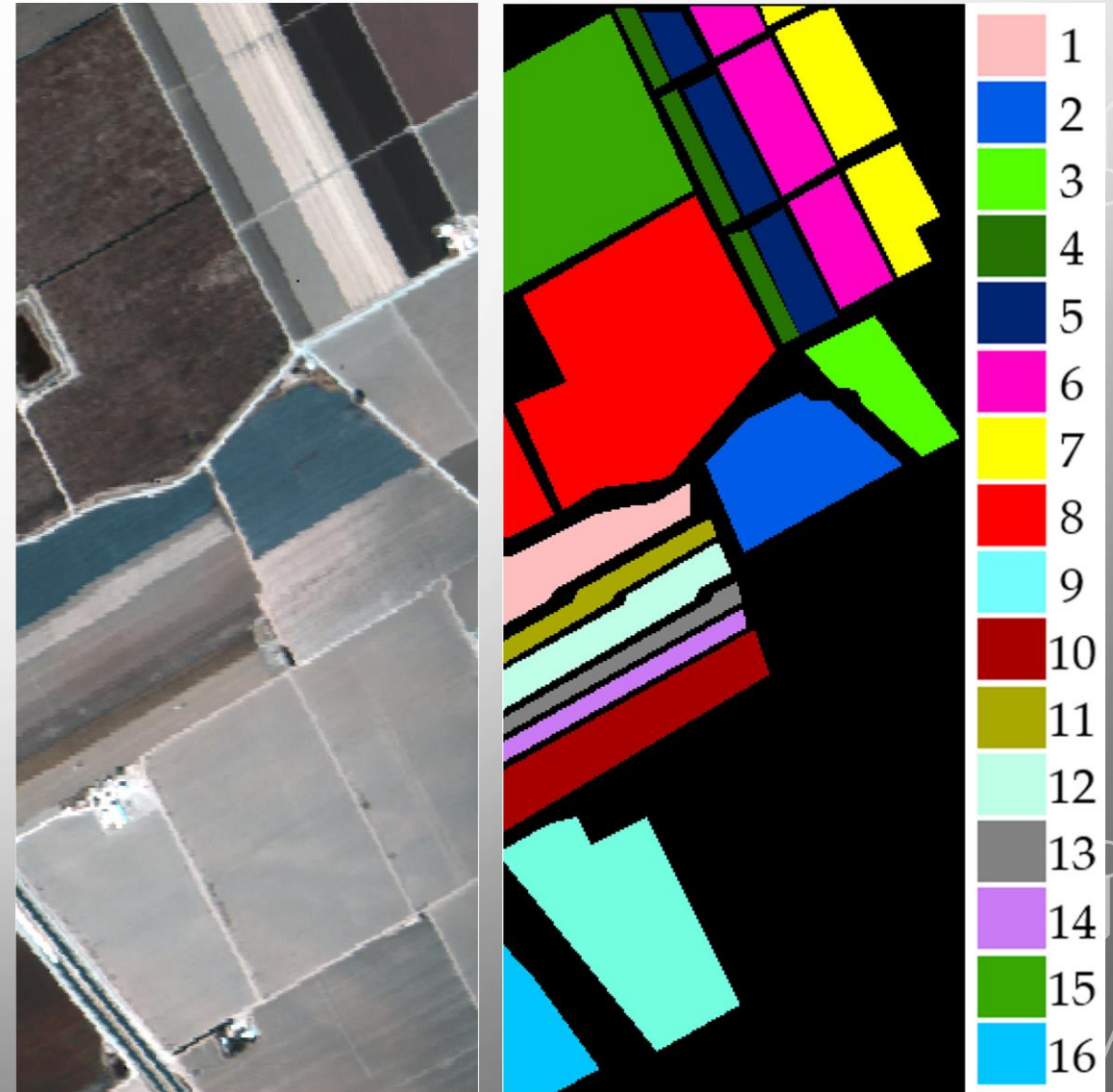


Figure 4. RGB composite and ground truth of the Salinas Scene.

2. HyRANK Loukia

- Developed by ISPRS WG III/4
- Obtained from EO-1 Hyperion sensor with 30 m spatial resolution and 220 bands.
- Only the Loukia data was considered in this study while HyRANK contains 5 HSI data.
- Contains 14 LULC classes.
- Final size of hypercube is $250 \times 1376 \times 176$.

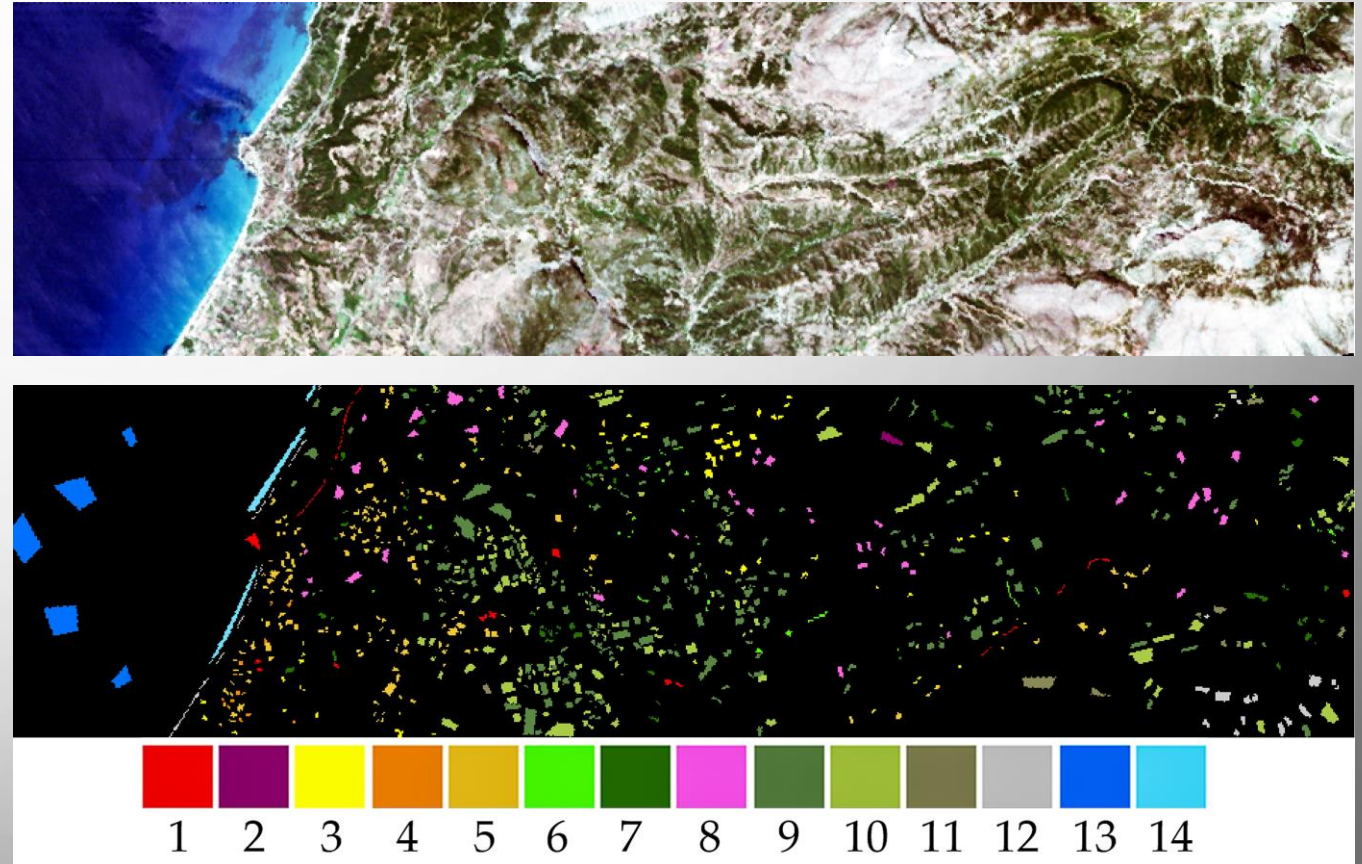


Figure 5. RGB composite and ground truth of the HyRANK Loukia.

Table 1. Number of train and test samples of the data sets.

	Salinas Scene Data Set			HyRANK Loukia Data Set		
#	Class Name	Train	Test	Class Name	Train	Test
1	Brocoli_green_weeds_1	150	1859	Dense urban fabric	150	138
2	Brocoli_green_weeds_2	150	3576	Mineral extraction sites	30	37
3	Fallow	150	1826	Non irrigated arable land	150	392
4	Fallow_rough_plow	150	1244	Fruit trees	30	49
5	Fallow_smooth	150	2528	Olive groves	150	1251
6	Stubble	150	3809	Broad leaved forest	150	73
7	Celery	150	3429	Coniferous forest	150	350
8	Grapes_untrained	150	11121	Mixed forest	150	922
9	Soil_vinyard_develop	150	6053	Dense sclerophyllous vegetation	150	3643
10	Corn_senesced_green_weeds	150	3128	Sparce sclerophyllous vegetation	150	2653
11	Lettuce_romaine_4wk	150	918	Sparsely vegetated areas	150	254
12	Lettuce_romaine_5wk	150	1777	Rocks and sand	150	337
13	Lettuce_romaine_6wk	150	766	Water	150	1243
14	Lettuce_romaine_7wk	150	920	Coastal water	150	301
15	Vinyard_untrained	150	7118			
16	Vinyard_vertical_trellis	150	1657			

4. RESULTS

- We built the classification models by using Python's Tensorflow, Keras and Scikit-learn libraries.
- C and γ parameters were determined for both datasets as 100 and 0.1 respectively with grid search.
- To compare the classification performances of the algorithms, we calculated overall accuracy (OA), producer accuracy (PA), user accuracy (UA), f scores, and kappa coefficient (κ).

Table 2. Performance analysis of the data sets.

Class ID	Salinas Scene data set						HyRANK Loukia data set					
	SVM			CNN			SVM			CNN		
	PA	UA	f score	PA	UA	f score	PA	UA	f score	PA	UA	f score
1	1.00	1.00	1.00	1.00	1.00	1.00	0.47	0.88	0.61	0.62	0.97	0.76
2	1.00	1.00	1.00	1.00	1.00	1.00	1.00	0.84	0.91	0.97	1.00	0.99
3	0.97	0.98	0.98	0.99	1.00	0.99	0.79	0.88	0.83	0.85	0.91	0.88
4	0.98	0.99	0.99	0.99	1.00	0.99	0.70	0.57	0.63	0.79	0.86	0.82
5	0.98	0.98	0.98	0.99	0.99	0.99	0.92	0.89	0.90	0.97	0.93	0.95
6	1.00	1.00	1.00	1.00	1.00	1.00	0.16	0.82	0.27	0.20	0.99	0.34
7	1.00	1.00	1.00	1.00	1.00	1.00	0.45	0.84	0.59	0.56	0.86	0.68
8	0.83	0.79	0.81	0.92	0.88	0.90	0.49	0.69	0.58	0.70	0.83	0.75
9	1.00	1.00	1.00	1.00	1.00	1.00	0.83	0.56	0.67	0.85	0.64	0.73
10	0.96	0.97	0.97	0.97	0.99	0.98	0.80	0.80	0.80	0.79	0.81	0.80
11	0.94	0.99	0.97	0.99	1.00	1.00	0.67	0.96	0.79	0.81	0.99	0.89
12	0.99	1.00	0.99	1.00	1.00	1.00	0.88	0.95	0.92	0.83	0.96	0.89
13	0.99	0.99	0.99	1.00	1.00	1.00	1.00	1.00	1.00	1.00	1.00	1.00
14	0.96	0.99	0.97	0.99	1.00	0.99	1.00	1.00	1.00	0.99	1.00	1.00
15	0.70	0.74	0.72	0.84	0.88	0.86						
16	0.99	1.00	0.99	0.98	1.00	0.99						
OA	91.36			95.68			76.37			81.38		
K	90.36			95.17			72.05			77.77		
time (s)	31.72			28.85			21.10			23.16		

- The CNN outperformed against SVM on both data sets.
- For Salinas Scene data set;
 - CNN has slightly better performance from SVM on 3rd, 4th, 5th, and 10th classes.
 - CNN has significantly higher accuracy on 8th and 15th classes.
 - SVM only showed slightly better performance according to PA on 16th class.
 - CNN's processing time is less than SVM's.
- For HyRANK Loukia data set;
 - In 2nd, 10th, and 15th classes, SVM's PA values are slightly higher than CNN's PA values.
 - PA of 1st, 6th, and 7th classes obtained a low value in the range from 0.16 to 0.62 for both classification algorithms, indicating that classification performance is considerably worse than other classes.
 - SVM's processing time is less than CNN's.

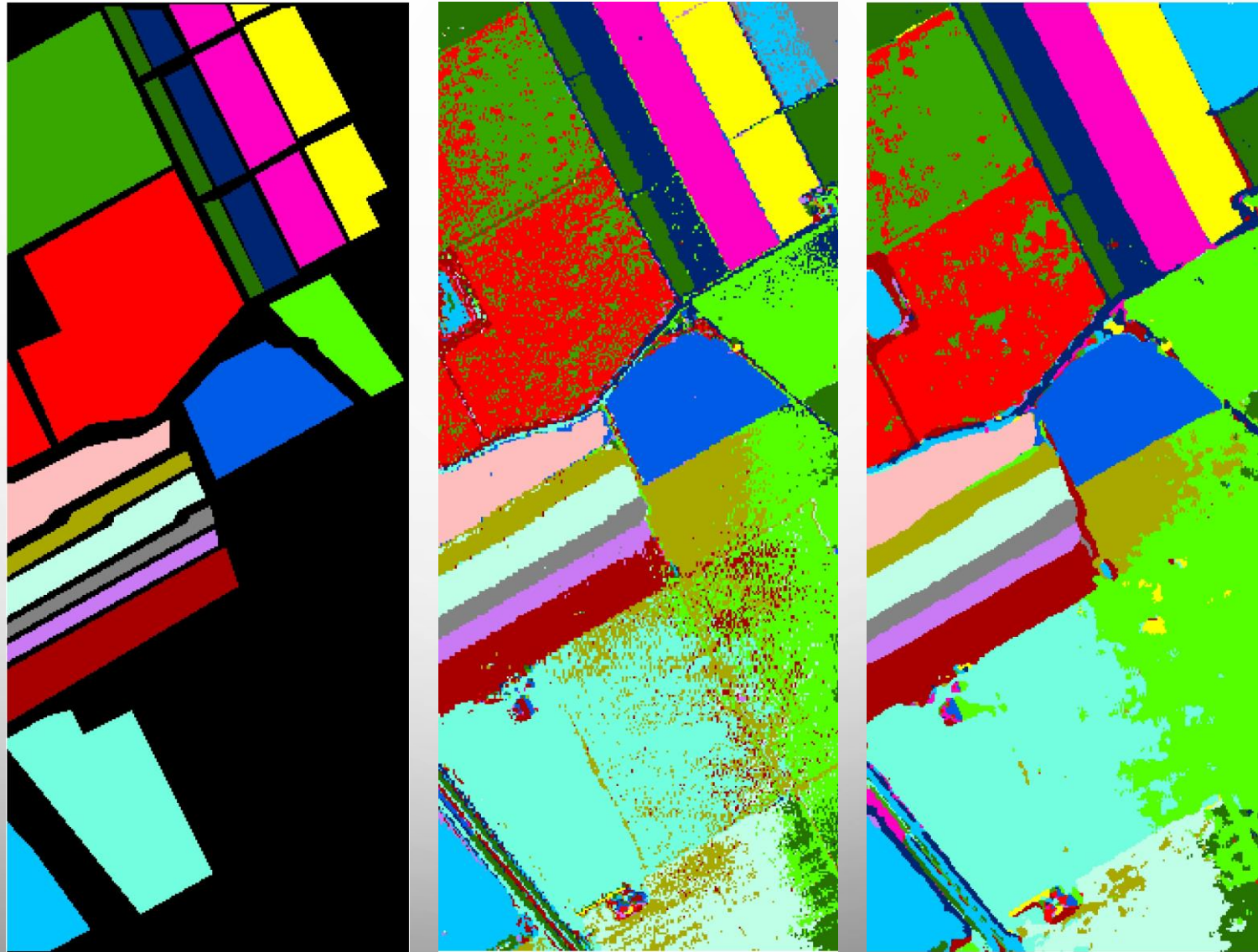


Figure 6. Ground truth, SVM classification map, and CNN classification map for Salinas Scene respectively.

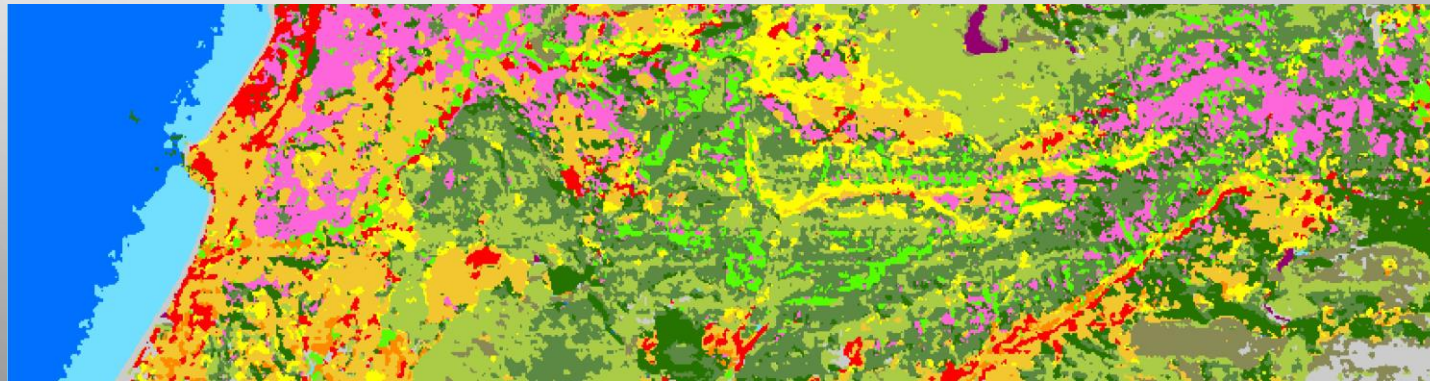
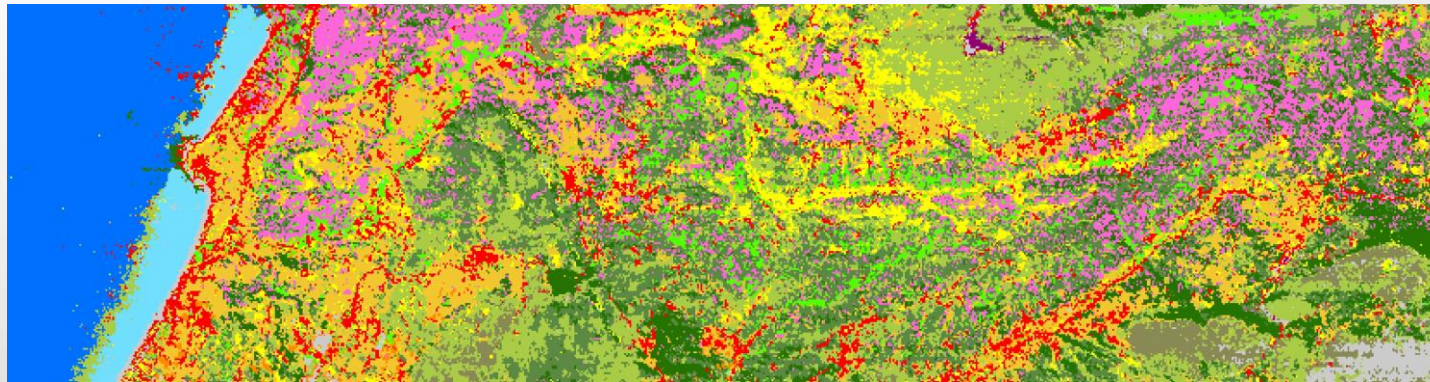
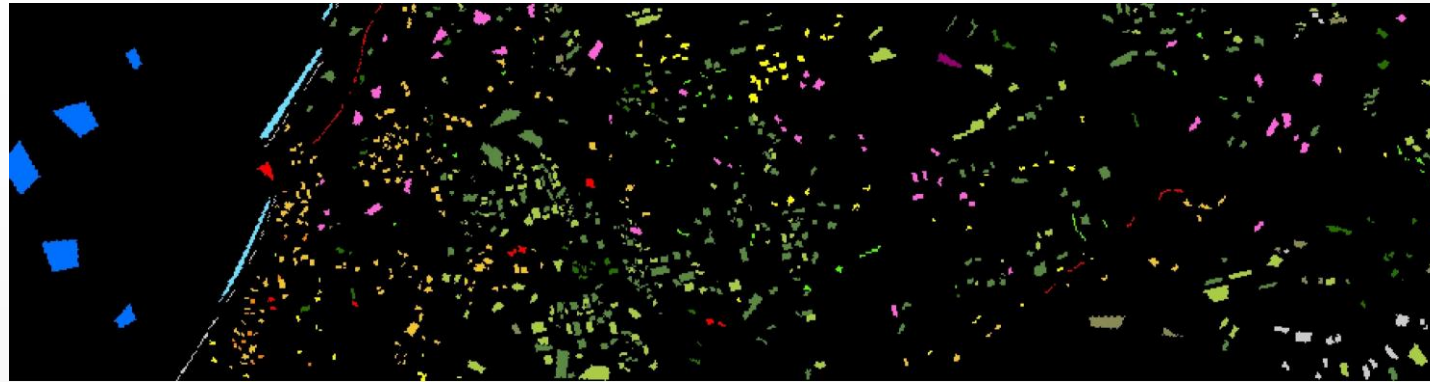


Figure 7. Ground truth, SVM classification map, and CNN classification map for HyRANK Loukia respectively.

5. CONCLUSIONS

- In this study, we evaluated the classification performances of HSI datasets with SVM and CNN algorithms.
- The experimental results shows that the CNN algorithm outperformed for both HSI data.
- For the SS data set, CNN showed a better performance by PA, UA and f scores against the SVM.
- For HL data set, CNN again gained better f scores in 10 of 14 land cover classes.
- Results showed that CNN models are useable on HSI classification problems that include agricultural and forestry areas.

Thank you.